PERGAMON

Microelectronics Reliability 40 (2000) 841–844

MICROELECTRONICS RELIABILITY

www.elsevier.com/locate/microrel

Growth of well-ordered silicon dioxide films on Mo(1 1 2)

T. Schroeder *, M. Adelt, B. Richter, M. Naschitzki, M. Bäumer, H.-J. Freund

Fritz-Haber-Institut der Max-Planck-Gesellschaft, Faradayweg 4-6, 14195 Berlin, Germany

Abstract

A preparation is reported which, for the first time, results in a thin, crystalline SiO_2 film on a Mo(1 1 2) single crystal. The procedure consists of repeated cycles of Si deposition and subsequent oxidation, followed by a final annealing procedure. LEED pictures of high contrast show a hexagonal, crystalline SiO_2 overlayer with a commensurate relationship to the Mo(1 1 2) substrate. AES and XPS have been used to control film stoichiometry. A spatial dependence of the Si^{4+} core level shift with distance from the interface plane is observed, but the shift is found to be essentially insensitive to the degree of crystallinity in the film. The wetting of the substrate by the film has been investigated by LEED, XPS and TDS. The results prove that the film covers the substrate completely. © 2000 Elsevier Science Ltd. All rights reserved.

1. Introduction

In semiconductor industry, the properties of SiO_2 and the SiO_2/Si interface are essential for the performance of electronic devices. New generations of metal oxide semiconductor field effect transistors (MOSFETs) require a scaling down of the thickness of the insulating SiO_2 layer [1]. One of the inherent problems in producing MOS gates in very large scale integrated circuits (VLSI) is reliability of the thin insulator layer. Therefore, a complete understanding of the SiO_2/Si interface is imperative. Decades of work clarified the key features, but there is still a considerable uncertainty in our knowledge of the details of the interfacial region. The SiO_2/Mo system shows similarities to the SiO_2/Si interface and offers the unique possibility to study the evolution of a thin, well-ordered SiO_2 film in the vicinity of a metallic interface.

2. Experimental

The film preparation starts with four cycles of the Si deposition, each followed by an oxidation step. Si is evaporated by electron bombardment of a Si rod, keeping the crystal at 300 K. The subsequent oxidation step is carried out at 800 K in an atmosphere of 5×10^{-5} mbar O_2 (6 min). Spectra taken during film deposition have been recorded after the oxidation step and are denoted according to the corresponding cycle (1–4). After the SiO_2 film deposition, four annealing steps are applied to order the film. The crystal is heated in an atmosphere of 5×10^{-6} mbar O_2 for 20 min, applying 1000 K during the first two and 1150 K during the last two annealing steps. Spectra taken during this preparation stage are denoted by the numbers 5–8, according to the respective annealing step.

3. Discussion

3.1. Crystallinity

Fig. 1 shows the result of our LEED study in terms of the clean Mo(1 1 2) surface (0), for reference, and the patterns obtained at the end of SiO_2 film deposition (4) and SiO_2 film annealing (8). The clean Mo(1 1 2) surface (0) exhibits a $p(1 \times 1)$ pattern, clearly indicating that the surface preserves the trough and row structure with its rectangular unit mesh expected from the bulk [2]. In the following, the spots at the position of the substrate spots will be referred to as the fundamental spots. SiO_2 film deposition results in the appearance of faint and streaky superlattice spots in the center of the rectangular substrate unit mesh which gain intensity with progress in

* Corresponding author.

0026-2714/00/$ - see front matter © 2000 Elsevier Science Ltd. All rights reserved.
PII: S 0 0 2 6 - 2 7 1 4 (9 9) 0 0 3 2 3 - 6

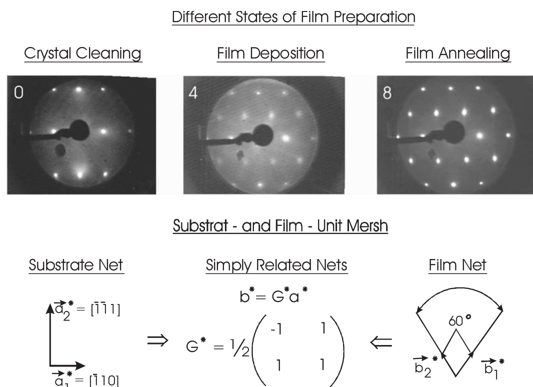

Fig. 1. Top: LEED pictures at $E = 56$ eV of clean Mo(1 1 2) (0), after SiO_2 film deposition (4) and after SiO_2 film annealing (8). Bottom: Sketches of the respective unit meshes and the epitaxial relationship.

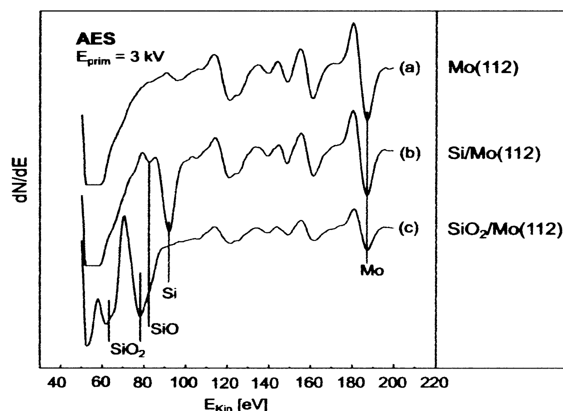

Fig. 2. AES spectra at different stages of the film deposition: (a) clean Mo(1 1 2), (b) Si deposition on clean Mo(1 1 2), and (c) SiO_2 film on Mo(1 1 2).

film deposition. At the end of the film deposition, the LEED pattern (4) consists of sharp fundamental and faint superlattice spots with a high background. Four annealing steps have been applied to order the film and the LEED pattern (8) shows the final result. The superlattice and the fundamental spots appear to have similar intensities now and the background is low, confirming the importance of the annealing steps to improve the crystallinity of the film. The film and substrate unit mesh are simply related and, thus, a commensurate growth of the hexagonal SiO_2 film on the rectangular Mo(1 1 2) surface is observed. The film unit mesh length is derived to be 5.2 Å.

3.2. Stoichiometry

3.2.1. Auger electron spectroscopy

Fig. 2 shows the differentiated AES spectra from 50 to 200 eV taken (a) for the clean Mo(1 1 2) substrate, (b) after depositing Si, and (c) at the end of the film preparation. The most intense peak in the AE spectrum from the Mo(1 1 2) surface is the $M_{4,5}NV$ transition at 187 eV [3]. The attenuation of this substrate peak is used to derive an estimate of the film thickness. All well-ordered SiO_2 films discussed here range in film thickness between 5 and 8 Å.

The deposition of Si leads to a strong feature at 92 eV which can be assigned to the $L_{2,3}VV$ transition of the elemental Si [4,5]. Due to the high reactivity of Si with respect to oxygen, a small signal is always visible at 84 eV, i.e. close to the position expected for SiO ($L_{2,3}VV$) [4,5]. At the end of the film preparation, i.e. after film annealing, the Si $L_{2,3}VV$ line shape is split into a main peak at 78 eV (Si $L_{2,3}V_1V_1$) and a satellite at 64 eV (Si $L_{2,3}V_2V_1$). This spectrum is in line with the reference spectra of silica samples, thus providing a first evidence for the successful preparation of a stoichiometric SiO_2 film on the Mo substrate [4,5].

3.2.2. X-ray photoelectron spectroscopy

XPS has the advantage that, via the Si_{2p} core level shift, the different Si oxidation states can be resolved [6]. In Fig. 3, various Si_{2p} (*left panel*) and O_{1s} photoelectron spectra (*right panel*) of SiO_2 acquired during the SiO_2 film deposition (1–4) and the SiO_2 film annealing (6 and 8) are presented. The upper inset shows the development of the position, the lower inset the evolution of the intensity. Note that the position of the elemental Si_{2p} photoelectron line on Mo(1 1 2) is found at 99.3 eV (not shown here).

During the SiO_2 film deposition (1–4), the intensity of the Si_{2p} photoelectron line scales linearly with the deposition cycles applied and decreases slightly (~15%)

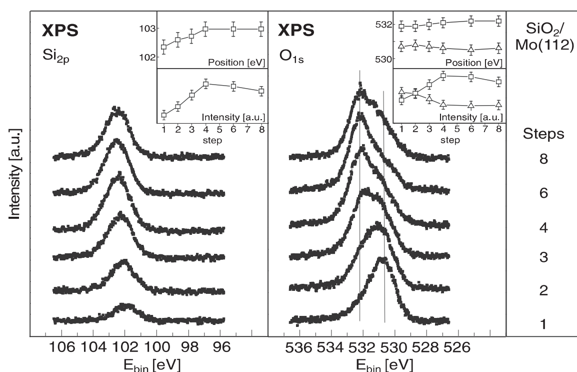

Fig. 3. Si_{2p} (left) and O_{1s} (right) photoelectron spectra recorded during SiO_2 film deposition (1–4) and SiO_2 film annealing (6, 8). The upper insets show the position, the lower insets, the intensity of the lines (□: Si_{2p} and O_{1s} signal from SiO_2; △: O_{1s} signal from oxygen chemisorbed on Mo(1 1 2)).

after the film annealing (6 and 8). Such a Si loss can be the consequence of SiO_2 evaporation from rough surface regions having a higher vapour pressure [7] or desorption of volatile SiO [8].

A further, more interesting point concerns the chemical shift of the Si^{4+} core level with the progress in the film preparation. During SiO_2 film deposition (1–4), a spatial dependence of the Si^{4+} core level shift with the film thickness is observed (chemical shift increasing from 3.1 eV after the first to 3.6 eV after the fourth deposition cycle). Note that this Si^{4+} core level shift merely depends on the film thickness, but not on the film order: SiO_2 film annealing (6, 8) results in a slight decrease of the FWHM from 1.8 to 1.7 eV, but no change in the position of the Si_{2p} signal is observed. The spatial dependence of the Si^{4+} core level shift with the film thickness is well known from the SiO_2/Si interface [9] and an explanation based on the dielectric discontinuity across the interface has been proposed here [10]. This seems to be a reasonable interpretation also in the present case as other reasons, such as charging effects [12], can be excluded due to the advantageous situation of studying the thin film on a metallic substrate. Structural aspects, as proposed by Grunthaner et al. [6], seem unlikely as well, because we can observe for the first time, the insensitivity of the Si^{4+} core level shift with respect to the degree of crystallinity in the film. This interpretation of our data is in line with the theory of the Si_{2p} core level shifts, developed for the SiO_2/Si interface [11].

The data further reveal that the growth of the SiO_2 film on Mo(1 1 2) is highly stoichiometric and differs from the SiO_2/Si interface by the absence of the Si suboxides, found in the transition region to adjust the density mismatch between the SiO_2 and Si lattice [13].

The O_{1s} photoelectron line in Fig. 3 consists of two peaks, which can be assigned to the oxygen chemisorbed at the interface to the Mo substrate (530.7 eV) [14] and to the oxygen, tetrahedrally coordinated to the Si (532.2 eV) [6], respectively. The peak at 530.7 eV decreases strongly with the SiO_2 film deposition, whereas the peak at 532.2 eV scales directly with the Si intensity, resulting in a Si : O ratio of approximately 2. The energy separation between O_{1s} and Si_{2p} signal is found to be 429 ± 0.4 eV, which is further indicative for SiO_2 [6].

3.3. Wetting behaviour

3.3.1. Low energy electron diffraction

It is worthwhile mentioning that the final LEED pattern (8) (Fig. 1) is already indicative of a high or a complete coverage of the substrate by the film. Whereas all the fundamental spots are sharp and isotropic, the superlattice spots are streaky with an anisotropic broadening along the a_2^* direction. This restriction of spot broadening to the superlattice spots points to the formation of antiphase domain boundaries within a continuous overlayer [15]. If the film covered only a part of the substrate, i.e. grew in islands, also the fundamental spots would be broadened [16].

3.3.2. X-ray photoelectron spectroscopy

In order to study the influence of the film preparation on the Mo substrate, Mo_{3d} spectra have been taken, which are presented in Fig. 4. A first set of spectra has been recorded during the different stages of the film preparation and, for reference, a second set without depositing any Si. This allows us to compare the behaviour of the Mo substrate under the preparation conditions with and without the film growth.

In the first case, the Mo signal is attenuated during film deposition (left panel of Fig. 4, steps 2 and 4), but regains intensity (~15%) during film annealing (steps 6 and 8). This is consistent with the observed Si loss (Fig. 3). It is noteworthy that no shift in the binding energy (BE) of the Mo_{3d} line can be detected throughout the whole procedure. Consequently, any oxidation of Mo or compound formation between Mo and Si can be excluded.

In the second case (see the right panel of Fig. 4), a strong intensity attenuation of the Mo_{3d} line can be observed as well, if the film deposition conditions (2 and 4) are applied. During the annealing steps (6, 8), the signal decreases further and finally reaches a saturation value. Although the shape and BE of the Mo_{3d} line do not alter during the first part of the preparation (2, 4), the appearance and the position of the XPS spectrum change drastically by applying film annealing conditions (6, 8). In fact, a fit procedure reveals that each spin–orbit component is now split into two components with an intensity ratio of approximately 1:2. Without going into details, such a spectrum is characteristic for MoO_2 [17]. As the uncovered substrate regions are obviously

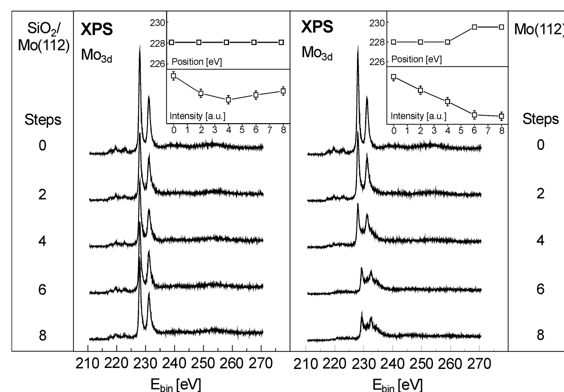

Fig. 4. Behaviour of the Mo_{3d} photoelectron line under film preparation conditions with a growing SiO_2 film (left panel) and without a growing SiO_2 film (right panel). The upper and lower insets show intensity and position of the line, respectively.

oxidized completely to MoO_2 under the film annealing conditions, the film coverage θ can be estimated by evaluating possible contributions of the MoO_2 spectrum to the spectrum of the SiO_2/Mo(1 1 2) system. By a peak fit procedure, using the line positions and the intensity distributions found for MoO_2 as the input parameters, a coverage of at least 95% can be calculated [18].

3.3.3. Thermal desorption spectroscopy

In order to tackle the question of film coverage in more detail, a TDS experiment based on the idea of selective chemisorption has been carried out. Deuterium (D_2) can be shown to adsorb on a clean Mo(1 1 2) [19] as well as on the oxygen-modified Mo(1 1 2) surfaces produced under conditions like those which are applied during the film preparation [18]. With SiO_2 not adsorbing D_2 above 100 K [20], the adsorption sites on the substrate become more and more blocked as the film grows. Indeed, a complete suppression of the strong D_2 uptake of the Mo(1 1 2) surface is observed in the experiment by deposition and annealing of the SiO_2 film [18]. Together with the experimental evidences reported above, this leads to the conclusion that a two-dimensional, continuous SiO_2 film is formed on the Mo(1 1 2) support.

4. Conclusion and outlook

The growth of SiO_2 on a Mo(1 1 2) single crystal results in a thin and well-ordered oxide film which is stoichiometric and continuous in nature. The spatial dependence of the Si^{4+} core level shift with distance from the interface is related to the dielectric discontinuity across the interface. No change of the Si^{4+} core level shift is observed by improving the film crystallinity, giving support to the theoretically predicted insensitivity of the Si^{4+} core level shift to the second and further neighbours in the structure [11]. The structure of the SiO_2 film has not been yet assigned to a particular phase, but further studies are under way.

References

[1] Muller DA, Sorsch T, Moccio S, Baumann FH, Evans-Lutterodt K, Timp G. Nature 1999;399:758–61.
[2] Braun O, Medvedev V. Sov Phys Usp 1989;32:328.
[3] Zhang C, Van Hove MA, Somorjai GA. Surf Sci 1984;149:326.
[4] Carriere B, Lang B. Surf Sci 1977;64:209.
[5] Carriere B, Deville JP. Surf Sci 1979;80:278.
[6] Grunthaner FJ, Grunthaner PJ, Vasquez R, Lewis B, Maserjian J, Madhukar A. J Vac Sci Technol 1979;16(5):1443.
[7] Markov I. Crystal growth for beginners. Singapore: World Scientific, 1995.
[8] Walkup R, Raider S. Appl Phys Lett 1988;53:888.
[9] Lu Z, Graham M, Jiang D, Tan K. Appl Phys Lett 1993;63:2941.
[10] Browning R, Sobolewski M, Helms C. Phys Rev B 1988;38:13407.
[11] Pasquarello A, Hypertsen M, Car R. Phys Rev B 1996;53:10942.
[12] Tao Y, Lu Z, Graham M, Tay S. J Vac Sci Technol B 1994;12(4):2500.
[13] Hollinger G, Himpsel F. Appl Phys Lett 1984;44(1):93.
[14] He J-W, Xu X, Corneille J, Goodman D. Surf Sci 1992;279:119.
[15] Libuda J, Winkelmann F, Bäumer M, Freund H-J, Bertrams T, Neddermeyer H, Mueller K. Surf Sci 1994;318:61.
[16] Tracy J, Blakely J. In: Somorjai GA, editor. The structure and chemistry of solid surfaces, New York: Wiley, 1969.
[17] Brox B, Olefjord I. Surf Interface Anal 1988;13:3.
[18] Schroeder T, Adelt M, Richter B, Naschitzki M, Bäumer M, Freund H-J. Surf Rev Lett (in press).
[19] Lopinski G, Prybyla J, Estrup P. Surf Sci 1993;296:9.
[20] Ko C, Gorte R. Surf Sci 1985;155:296.